



CODEN [USA]: IAJPBB

ISSN : 2349-7750

**INDO AMERICAN JOURNAL OF
PHARMACEUTICAL SCIENCES**

SJIF Impact Factor: 7.187

Available online at: <http://www.iajps.com>

Research Article

**COBALT OXIDE NANOPARTICLES: SYNTHESIS AND
CHARACTERIZATION****Veronica Deekala¹, Rathna Babu Guntur¹, Jyothsna Pragathi Yazala¹,
Anitha Kowthalam², Ramesh Raju Rudra Raju¹**¹ Department of Chemistry, Acharya Nagarjuna University,
Nagarjuna nagar-522510² Department of Chemistry, Sri Krishnadevaraya University, Ananthapur, 515003.**Article Received:** August 2021**Accepted:** September 2021**Published:** October 2021**Abstract:**

The cobalt oxide Nanoparticles were synthesized from Cobalt Nitrate Hexahydrate aqueous solution under the chemical method at 60-90°C. The average crystallite size was calculated from De-Bye Scherrer's equation. FESEM, EDX, XRD were used to characterize the structural features of the product. FTIR spectra confirmed the adsorption of the cobalt oxide nanoparticles. In addition, UV-visible absorption spectra were employed to estimate the band gap energy of the copper oxide nanoparticles. This method may be suitable for large scale production of cobalt oxide nanoparticles for practical applications. The effect of cobalt oxide nanoparticles is screened in vitro for antimicrobial activity by Disc diffusion method. The bacterial organisms used in this study are E.coli, Bascillus Subtilis. The observed inhibition zones for these nanoparticles are in the range of 22mm for E.coli and 20mm for Bascillus Subtilis. The cytotoxicity activities of copper oxide nanoparticles screened by MTT-assay. We have screened for one type of cancer cell-line i.e MCF-7(Breast Cancer), cobalt oxide nanoparticles obtained IC₅₀ values in the range of 54ug/ml for MCF-7 cell line.

Keywords: Cobalt Oxide Nanoparticles, SEM, EDX, XRD, FTIR, UV-Vis, Disc diffusion method, Cytotoxicity.**Corresponding author:****Ramesh Raju Rudra Raju,**

Department Of Chemistry, Acharya Nagarjuna University,

Nagarjuna nagar-522510.

Email: rrraju1@gmail.com

QR code



Please cite this article in press Veronica Deekala et al, Cobalt Oxide Nanoparticles: Synthesis And Characterization., Indo Am. J. P. Sci, 2021; 08(10).

INTRODUCTION:

These nanocrystals display a wealth of size-dependent structural, magnetic, electronic and catalytic properties. It is difficult to make isolated cobalt nanoparticles without a surfactant, in part because the forces between particles are large. The Cobalt synthesis is also used for magnetic storage purpose due to high magnetic relaxation time on volume. The Cobalt nanoparticles are having a high covalent bonding which gives an enhanced stability of nanoparticles.

MATERIALS:

All of chemicals used in experiment are of analytical grade and used as purchased without any purification. Cadmium hexahydrate $\text{Co}(\text{NO}_3)_2 \cdot 6\text{H}_2\text{O}$, of 98% purity is used. De-ionized water used as a solvent. Sodium hydroxide (NaOH) is used to adjust the pH.

Cobalt nitrate hexahydrate $\text{Co}(\text{NO}_3)_2 \cdot 6\text{H}_2\text{O}$ and sodium hydroxide NaOH were each dissolved separately in deionized water to form the liquid media of the desired concentrations of 0.05M (2.3g/250mL) and 0.1M (1g/250mL) for sample A and B respectively the ratio of the concentrations was 1:1 ($\text{Co}(\text{NO}_3)_2 \cdot 6\text{H}_2\text{O}$: NaOH). The cobalt nitrate hexahydrate was slowly added drop-wise to NaOH solutions under vigorous stirring at room temperature, forming transparent white solutions, then inserted into an electrical oven at 60-90°C for 2 hours. These solutions were reacted to produce cobalt oxide precipitates. Following the precipitation, the solution was centrifuged at 3000 rpm for 30 minutes. The supernatant was then removed, and the precipitation which contains cobalt oxide was obtained. Finally, cobalt oxide was grinded with mortar to be shaped into powder.

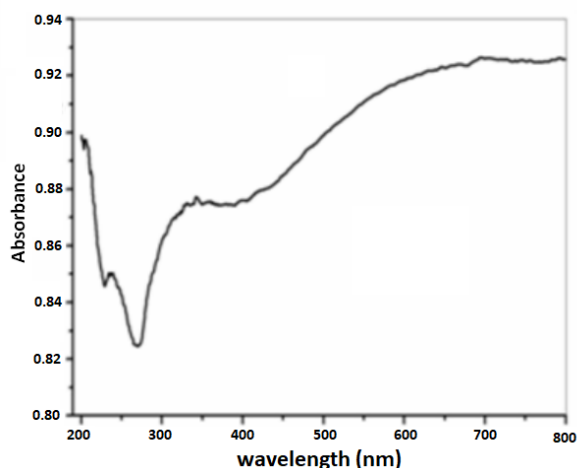
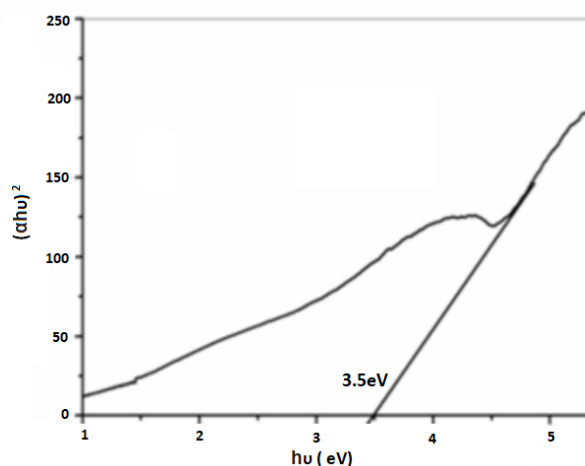
Synthesis of cobalt oxide Nanoparticles**Optical characterization:**

Fig.1. (a) UV-absorbance spectra of cobalt oxide (Co_3O_4), (c) DRS band gap of cobalt oxide (Co_3O_4)

Fig.1.(a) shows the absorbance at 250 to 350 cm^{-1} and 400-580 cm^{-1} , the first absorption at due to O^{2-} to Co^{2+} the ligand to metal charge transfer and the band at 580 cm^{-1} corresponds to O^{2-} to Co^{3+} charge transfer [2]. The cubic phase Co_3O_4 behaves as a p-type semiconductor. The spectrum can be explained in terms of charge transfer in transition metal (TM) oxides. The relationship between the absorption coefficients α is an incident photon energy $h\nu$. In order to calculate the optical band gap of sample by using Tauc's relation in Eq.(2)

$$(\alpha h\nu)^n = A(h\nu - E_g) \dots \dots \dots (2)$$

Where α denotes the absorption coefficient, A is

constant, E_g is band gap and exponent n depends on the type of transition. Fig.1.(b) shows the optical band gap was calculated using Tauc relation by plotting $(\alpha h\nu)^2$ against $h\nu$, by extrapolating the curve to photon energy axis. Calcium cobaltite prepared in this work, cobalt exists in the octahedra of oxygen ions with Co^{3+} ions occupying tetrahedral and octahedral sites, respectively. Hence the optical energy band gap at $E_g=3.5\text{eV}$, due to the electron creates positive hole in the valence band to the conduction band. Hence d-d charge transfer takes place in the Co_3O_4 system it shows p-type semiconducting material.

FTIR Spectrum of copper oxide Nanoparticles:

Fig.2 shows FTIR spectra of Co_3O_4 nanoparticles. Infrared studies were carried out in order to ascertain the purity and nature of the metal nanoparticles. Metal oxides generally give absorption bands in fingerprint region i.e. below 1000 cm^{-1} arising from inter-atomic vibrations.

The peak observed at 3461.10 and 1384.08 cm^{-1} are may be due to O-H stretching and deformation, respectively assigned to the water adsorption on the metal surface. The peaks at 1637.08 , 623.10 cm^{-1} are corresponding to Co_3O_4 stretching and deformation vibration, respectively.

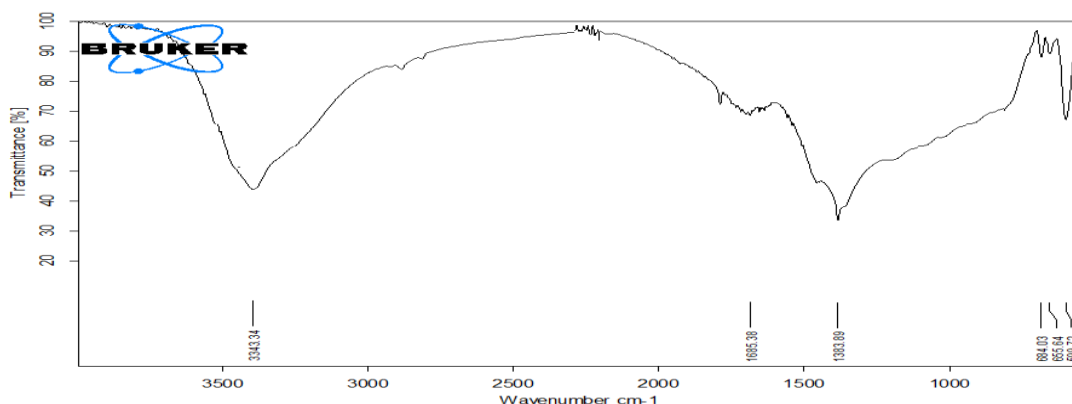


Fig.2. Shows the FT-IR spectrum of the Co_3O_4 nanoparticles

Table.1. Comparison of Vibrational modes of Co_3O_4 nanoparticles

S.No	Co_3O_4 (cm^{-1})	Vibrational modes
1	3461.10	OH
2	1384.08	OH deformation
3	623.10	Stretching of Co_3O_4
4	1637.08	C-H

Powder XRD analysis:

Fig.3 shows XRD diffraction pattern of Co_3O_4 nanoparticles. The peaks are indexed as 26.85° (220), 30.63° (311), 33.29° (222), 44.96° (400), 56.37° (422) and 58.32° (400) respectively. All diffraction peaks of sample correspond to the characteristic hexagonal

wurtzite structure of Co_3O_4 nanoparticles. Average particle size of Co_3O_4 nanoparticles is found to be 10.0 nm using Scherrer equation³⁷. Diffraction pattern corresponding to impurities are found to be absent. This proves that pure Co_3O_4 nanoparticles were as synthesized.

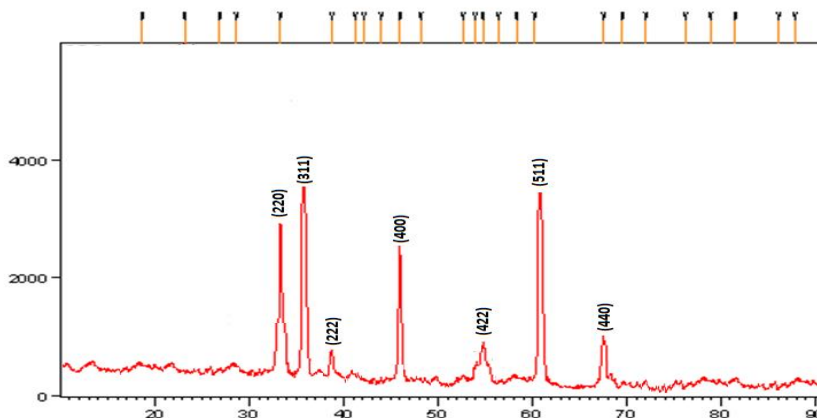


Fig.3. XRD patten of Co_3O_4 nanoparticles

Interplanar d-spacing was calculated using Bragg's Law equation (Table 2):

$$2d \sin\theta = n \lambda \dots\dots\dots (2)$$

where, θ is Bragg's angle of diffraction, λ is X-ray wavelength, i.e. 1.5406 \AA and $n = 1$. Further, particle size was calculated from the intense peak corresponding to (101) plane using Scherrer formula

$$D = 0.89\lambda / \beta \cos\theta \dots\dots\dots (3)$$

Where $0.89 =$ Scherrer's constant, $\lambda =$ X-ray wavelength (1.5406 \AA), $\beta =$ FWHM (Full Width at

Half Maximum) of the peak located at $2\theta = 36.27$ and $\theta =$ Bragg's angle of diffraction. The value of particle size was found to be 16.78 nm .

Field emission Scanning Electron Microscope (FESEM):

FE-SEM image Fig.4 shows the surface morphology and particle size of the synthesized Co_3O_4 nanoparticles. It is clear from the images that the size of the Co_3O_4 nanoparticles is ranging from $24\text{-}26 \text{ nm}$. The obtained products are composed of nearly flower shaped morphology with average size in the range of 50 nm .

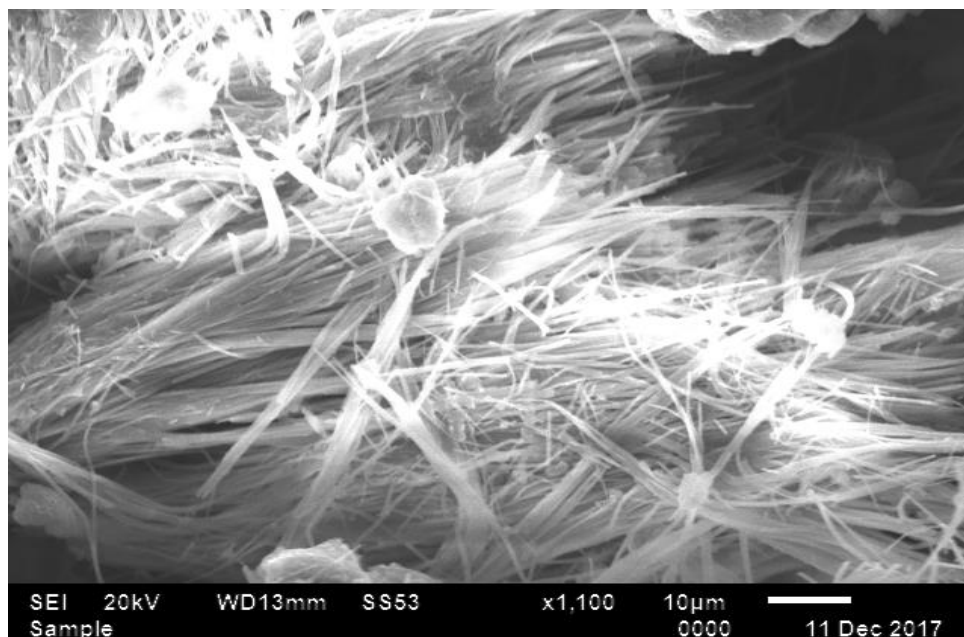


Fig.4. Shows the Field emission Scanning Electron Microscope (FESEM)

Energy Dispersive X-ray Spectroscopy (EDX):

The Energy dispersive X-ray Diffractive (EDX) study was carried out for the synthesized Co_3O_4 nanoparticles (Fig.6) to know about the elemental composition. EDX confirms the presence of element cobalt and oxygen signals of Co_3O_4 nanoparticles and this analysis showed the peaks that corresponded to

the optical absorption of the produced nanoparticles. The elemental analysis of the nanoparticles yields 86.95% of cobalt and 13.05% of oxygen which proves that the produced nanoparticles is in its highest purified form and was in agreement with the earlier studies [5].

Element	Weight%	Atomic%
O K	13.05	31.27
Co K	86.95	68.72
Totals	100	

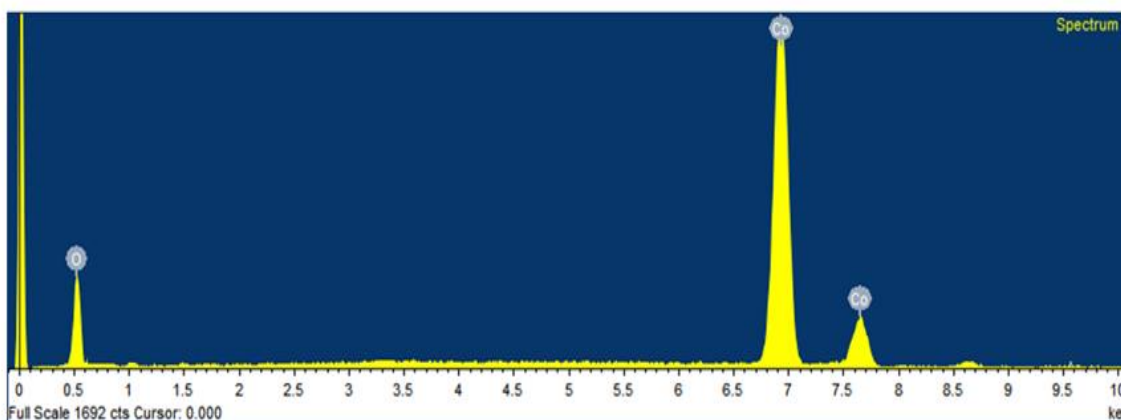
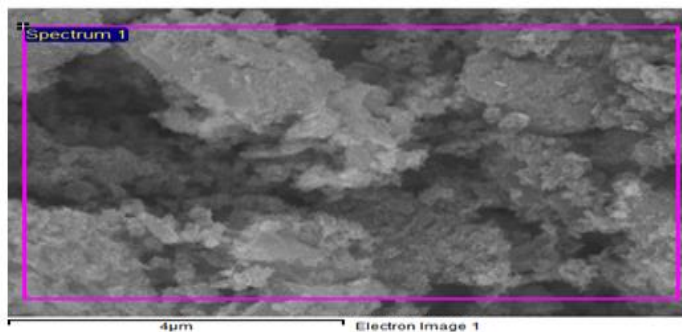


Fig.5. EDX of Co_3O_4 nanoparticles

Antimicrobial Screening of Co_3O_4

The Co_3O_4 nanoparticles are screened invitro for anti-bacterial activity against E.coli, B.subtilis and

antifungal activity against A.niger by Agar-well diffusion method. The anti-bacterial and antifungal activities of Co_3O_4 nanoparticles are listed in table.

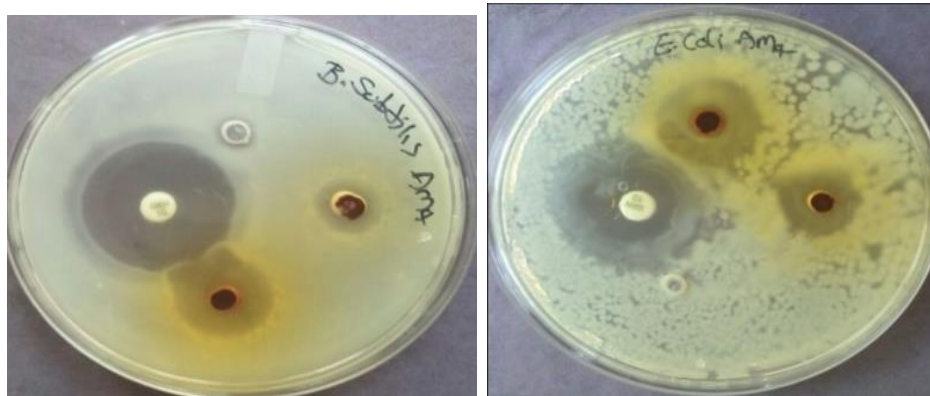


Fig .6. Inhibition zones for Co_3O_4 nanoparticles against. B.subtilisE.coli



Fig.7. Inhibition zones for Co_3O_4 nanoparticles against *A.niger*

Table.2. Antimicrobial activities of Co_3O_4 nanoparticles

Bacteria	Inhibition zone (mm)
E.coli	22
B.subtilis	20
Fungi	Inhibition zone (mm)
A.Niger	12

The Co_3O_4 nanoparticles showed good antibacterial activity against *E.coli* and *B.subtilis* and anti-fungal activity against *A.niger*.

Cytotoxic studies of Co_3O_4 nanoparticles

The fused Co_3O_4 nanoparticles are screened for their cytotoxicity (MCF-7, cell lines). From the data, it is observed that the Co_3O_4 nanoparticles displayed their cytotoxic activities as IC_{50} ($\mu\text{g}/\text{mL}$) against breast cancer MCF-7[25-55] The IC_{50} values of the Co_3O_4 nanoparticles are listed in table.

Table.3. Dose response of Co_3O_4 nanoparticles on MCF-7 cell line

Conc($\mu\text{g}/\text{ml}$)	% cell survival	% cell inhibition
0.1	88.83086	11.16914
1	87.34431	12.65569
10	77.90277	22.09723
100	22.61953	77.38047

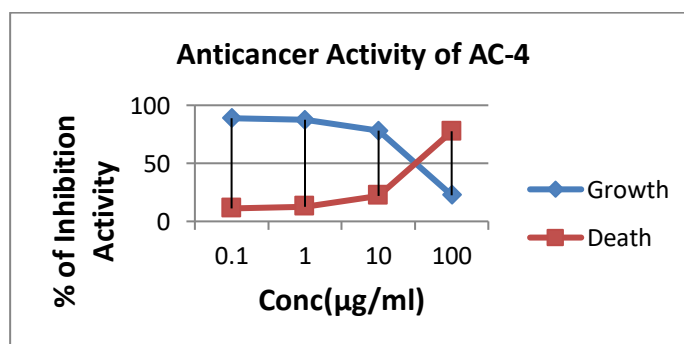


Fig.8. Effect of Co_3O_4 on MCF7 Cell viability for 24h Incubation time

IC50

54.45 $\mu\text{g}/\text{mL}$

CONCLUSION:

In the present study on synthesis of Cobalt oxide nanoparticles using chemical method and their antimicrobial activity, Cobalt oxide nanoparticles were synthesized using Cobalt nitrate hexahydrate. Synthesis conditions were optimized and resultant nanopowder was characterized using UV-Visible spectroscopy, XRD, FESEM. Morphological analysis report particle size range of 50 nm and also revealed that the nanoparticles are present in the form of aggregates. While studying the effect of nanoparticles for their antifungal potential, these showed activity against 2 bacterial pathogens and 1 fungal pathogen. It could be utilized for developing antifungal agents for commercial use in the field of agriculture. This study conclusively reports a synthesis of Cobalt oxide nanoparticles. Such studies have the potential for developing good fungicidal formulations having nanoparticles. The cytotoxicity activities of Cobalt oxide nanoparticles screened by MTT assay. We have screened for one type of cancer cell line, viz., MCF-7 (breast cancer), zinc oxide obtained IC₅₀ values in the range of 54.45µg/mL for MCF-7 cell line most of these nanoparticles are in cytotoxic activity.

REFERENCES:

1. Moon, J., Kim, T.K., Saders, B., Choi, C., Liu, Z., Jin, S and Chen R, *Sol. Energ. Mat.*, Sol. **2015**,134, 417–424.
2. Zheng, Y., Li, P., Li, H and Chen, S., *Int. J. Electrochem. Sci.* **2014**, 9,7369 – 7381.
3. Sun,H., Ahmad, M and Zhu, J. *Electrochim Acta* **2013**,89, 199 – 205.
4. Madhu, R., Veeramani, V., Chen, S., Manikandan, A., Lo, Y and Chueh, L., *ACS Appl. Mater. Interfaces*, **2015**, 29,15812-20.
5. Cao, Y., Yuan, F., Yao, M., Bang, J.H and Lee, H., *J. Cryst. Eng., Comm*, **2014**,16, 826–833.
6. Xu, J., M, Zhang, J., Wang, B and Liu F. J. *Alloys Compd.* **2015**,619, 361– 367.
7. Sahoo, P., Djieutedjeu, H and Poudeu, Pierre. J. *Mater. Chem.* **2013**,1, 15022- 15030.
8. Niasari, M.S., Mir, N and Davar, F. J. *Phys. Chem. Solids*, **2009**,70,847–852.
9. Makhlof, S.A., Bakr, Z.H., Aly, K., Moustafa, M.S., *Superlattices and Microstructures.* **2013**, 64, 107– 117.
10. Nandapure, B., Kondawar, S., Nandapure, A, *Int. J. Sci. Res.* **2015**,4(1), 440- 441.
11. Rathod, P., Nemade, K and Waghuley, S. *Int. J. Chem. Phys. Sci.* **2015** 4, 491- 95.
12. FarhadiSaeed., Sepahdar Asma and Jahanara Kosar. *J. nanostruct.* **2013**, 199- 207.
13. Al-Tuwirqi, R., Al-Ghamdia., A., Aal., Umar, A and Mahmoud, W.E., *Superlattices and Microstruct.* **2011**, 49, 416–421.